Desalination and Water Treatment
www.deswater.com
doi: 10.5004/dwt.2019.23182

137 (2019) 125–133
January

Silica nanoparticles for the removal of fluoride from aqueous solution: equilibrium, isotherms, kinetics, and thermodynamics

Fatemehsadat Masoudi[a], Ali Naghizadeh[b,*]

[a]*Student Research Committee, Faculty of Health, Birjand University of Medical Sciences (BUMS), Birjand, Iran, Tel. +985632381665; Fax: +985632395346; email: Ftmmasoudi71@yahoo.com*
[b]*Medical Toxicology and Drug Abuse Research Center (MTDRC), Birjand University of Medical Sciences (BUMS), Birjand, Iran, Tel. +985632381665; Fax: +985632395346; email: al.naghizadeh@yahoo.com*

Received 13 February 2018; Accepted 24 September 2018

ABSTRACT

Fluorine is one of the most active and electronegative elements of the periodic table that exists in different amounts and sizes in water, soil, and plants. The excessive use of this substance can cause many problems. The research work was an experimental laboratory study aimed to investigate the fluoride removal from aqueous solutions by silica nanoparticles. The effect of different variables such as pH (3–11), adsorbent dose (0.2–2 g/L), contact time (2–120 min), different concentrations of fluoride (2–10 mg/L), and temperature (283, 293, 303, and 313 K) were determined in batch condition. Also, kinetics, thermodynamics, and isotherms process were studied. The results of this study showed that maximum adsorption capacity in optimum conditions (pH = 3, the adsorbent dose of 0.2 g/L, the contact time of 10 min, and the initial concentration of 10 mg/L) was found to be 8.40 mg/g. Also, the adsorption process was an endothermic and spontaneous as well as the Dubinin–Radushkevich isotherm and pseudo-second-order kinetic is more consistent with adsorbing fluoride by the silica nanoparticles. This study indicated that silica nanoparticles can be used in optimum conditions as an effective, usable and inexpensive adsorbent for the fluoride removal in aqueous solutions which values are higher than the standard level.

Keywords: Adsorption; Fluoride; Silica nanoparticles; Kinetics; Thermodynamics

1. Introduction

Today, one of the health concerns about the quality of drinking water is the high amount of fluoride due to factors such as contact with mineral stones containing fluoride and its dissolution in water. In groundwaters, high fluoride concentrations are due to the large and extensive belts associated with granitic and volcanic rocks and fluoride minerals [1]. The fluoride ion has a degree of oxidation (–1), it is pale yellow and has a high toxicity and corrosion which due to its high reactivity, it cannot be found freely in nature, and is commonly found in a number of mineral compounds such as fluorescence (fluorite), cryolite (sodium fluoride and aluminum), and fluorapatite [2–4].

The United States Public Health Organization has recommended an optimal concentration of fluoride in water (1.2–0.7 mg/L), and the WHO has also stated a limit of 1–1.5 mg/L [3,5]. By human advancement and industrial activity increases, more fluoride inters the environment. Industries, such as electroplating, metal processing, glass making and the production of semiconductors, and fertilizers, with the use of fluoride compounds, cause fluoride to enter the environment through the disposal of wastewater [6].

Drinking water is the main source of fluoride entry into the body, the concentration of fluoride in drinking water in the lower than standard levels causes tooth decay and, in excess of the standard, results in a decrease in calcium from the tooth root and the formation of dental fluorosis and also

* Corresponding author.

leads to a change in DNA structure and damage to the endocrine, thyroid, liver, softening of the bones, bone tendons and ligaments, reduced internal space between the spine and loss of empowerment, infertility in women, Alzheimer's disease, and brain damage [3,7,8].

Fluoride contamination is a global problem, especially in Africa, Asia, and the United States [9,10]. Studies have shown that the concentration of fluorine in groundwater in more than 22 developed and developing countries, including Iran, is higher than the recommended values of the World Health Organization [11]. Available statistics show that more than 30 million people in China are seriously influenced by fluorosis and another 100 million people are in danger [12]. In some cities in Iran, the fluoride content of drinking water is higher than 1.5 mg/L, which can lead to fluorosis and other problems [13]. Due to the adverse health effects of excessive fluoride in water the importance of removing this ion from water sources is significant. Studies show that various methods, such as adsorption process [14], chemical deposition [15], ion exchange, electrode dialysis [16], reverse osmosis [17], and nanofiltration [18–20], are used to remove excess fluoride from water sources. Among these methods, the adsorption process has been considered as a common, easy, and economical way to remove fluoride from aquatic environments [21,22].

In the study of Xiaotian X et al., manganese-coated ash in fluoride removal, the highest adsorption capacity was 6 mg/g at PH = 3 and the adsorbent dose was 2.5 g/L [23]. In a study of Vinitnantharat et al. [24] titled removal of fluoride ion in aqueous solutions by adsorption on acid activated water treatment sludge, reported that with an increase in adsorbent dose from 5 to 50 g/L, the removal efficiency increased from 40% to 73%. And also the adsorption capacity is increased at pH below 6.5 [24]. Nanoparticles have been widely used as adsorbent in removing pollutants from aqueous solutions due to its high surface area and adsorption capacity [25,26]. SiO_2 is structurally similar to the structure of the water molecule and it composed of two elements of silicon and oxygen and. SiO_2 is a major component of soil that is used to grow bacteria due to its lack of toxicity as a base material. Studies have shown that SiO_2 nanoparticles can be used as adsorbents for the removal of natural contaminants and metal ions [27,28]. Moriguchi et al. used modified silica nanoparticles for the removal of humic acid and folic acid and pH = 3 as optimal pH under optimal were obtained. Also, adsorption conditions with 2 mg/L adsorbent at 7.6 mg/L of humic acid and folic acid solution, 97%–93% removal of humic acid and 80%–86% removal of folic acid were reported [29]. Syed et al. in a study on the treatment of oily water using hydrophobic nano-silica showed that silica nanoparticles were effective at the natural pH of water and room temperature to remove oil and gasoline [30]. In a study conducted by Banerjee et al. [31], silica nanoparticles were reused as catalyst. The ultrasound method was also used for regeneration of carbon nanotubes and grapheme nanoparticles [32,33]. So far, many studies have been carried out on the removal of fluoride from aqueous solutions by various adsorbents. However, there were not many studies about removal of fluoride by silica nanoparticles. The purpose of this study was to use silica nanoparticles in water purification and removal of ion fluoride and finally the effect of different factors (such as pH, initial fluoride concentration, adsorbent amount and isotherm, kinetics, and thermodynamic studies) in batch flow were investigated.

2. Materials and methods

This study was an experimental study that was performed continuously on kinetic samples by changing a parameter and maintaining other parameters. In this study, silica nanoparticles with a 99.9% purity and a special surface area of 200 m^2/g applied as adsorbent. The NaF salt made by the German company (Merck) with a purity of 98.5%–100.5% was used to make stoke fluoride.

For this purpose, specific amount of salt was dissolved in deionized water and then the synthetic fluoride solutions were prepared by diluting the stock solution at initial fluoride concentrations. The effect of parameters such as pH (3, 5, 7, 9, and 11), adsorbent dose (0.2, 0.5, 1, 1.5, and 2 g/L), initial fluoride concentrations (2, 5, 8, and 10 mg/L), contact time (2, 5, 10, 20, 40, 60, 90, and 120 min), and temperature (283K, 293K, 303K, and 313K) on the removal of fluoride by the adsorbent was investigated. The pH meter (HACH made in America) was used to determine the pH and the NB-101MT was used to mixing samples. Also, for the effect of temperature on the samples, a SI-100R incubator shaker made in Korea was used. To adjust the acidity of 1 and 0.1 normal solution of NaOH and HCL was used. The nanoparticles from the final specimens were separated by acetate cellulose filter paper. To measure the residual fluoride concentration, the DR6000 Spectrophotometer was used according to Method 8029 guideline.

Finally, the adsorption capacity of silica nanoparticles was calculated by Eq. (1) [34,35]:

$$q_e = \left(\frac{C_0 - C_e}{M}\right) \times V \tag{1}$$

where q_e: the adsorption capacity (mg/g), C_0: initial concentration of fluoride in solution (mg/L), C_e: fluoride equilibrium concentration (mg/L), V: sample volume (L), and M: mass of silica nanoparticles (g).

2.1. Adsorption process isotherms

The isotherm determines the relationship between the amount of adsorbent material and the adsorbing material. In this study, for the mathematical modeling of the fluoride adsorption process, various nanoparticles of various silica isotherms were investigated.

2.1.1. Freundlich isotherm model

The linear form of this isotherm shows by Eq. (2):

$$\log q_e = \log K_F + \frac{1}{n} \log C_e \tag{2}$$

where C_e: equilibrium concentration (mg/L) and q_e: amount of dye adsorbed on adsorbent (mg/g). n and K_F are Freundlich constants[36].

2.1.2. Langmuir isotherm model

The linear model of Langmuir isotherm shows in Eq. (3):

$$\frac{C_e}{q_e} = \frac{1}{q_m K_L} + \frac{C_e}{q_m} \tag{3}$$

where C_e: equilibrium concentration (mg/L) and q_e: amount of dye adsorbed on adsorbent (mg/g), q_m: the maximum amounts of fluoride adsorbed (mg/g), and K_L: the Langmuir isotherm constant (L/m) [20,36].

2.1.3. BET isotherm model

The Brunauer–Emmett–Teller (BET) equation is as follows:

$$\frac{C_e}{q_e\left(C_s - C_e\right)} = \frac{1}{K_b q_{\max}} + \frac{K_b - 1}{K_b q_{\max}} \times \frac{C_e}{C_s} \tag{4}$$

where C_s: the saturation concentration of the soluble matter in mg/L, K_b: the constant obtained through the equation of the line, expresses the energy between the adsorbed material and the surface of adsorbent and is directly related to the adsorption energy; $q_{\max}$: the amount of adsorbed material per unit mass of the adsorbent (g) to form a single molecular layer on the adsorbent (mg/g) [36].

2.1.4. Temkin isotherm model

Temkin isotherm equation is as follows:

$$q_e = B \ln A_T + B \ln C_e \tag{5}$$

where $B = RT/b_T$, R is the universal gas constant (8.31 J/K/mol) and T is the absolute temperature (K).

Regarding to the isotherm curves, B and A are the slope and intercept of the curve, respectively. A_T: the equivalent constant of the bond associated with the maximum binding energy (L/mg), b_T: Temkin constant is proportional to the heat of adsorption (J/mol) [37].

2.1.5. Dubinin–Radushkevich (D–R) isotherm model

The linear equation of this isotherm is expressed as follows:

$$\ln q_e = \ln q_m - \beta\varepsilon^2 \tag{6}$$

$$\varepsilon = RT \ln\left(1 + \frac{1}{C_e}\right) \tag{7}$$

where T is the absolute temperature and R is the universal gas constant, q_e: the amount of matter dissolved per unit mass of adsorbent and q_m: the capacity of single-layer adsorption. The β coefficient (mol^2/kJ^2) is a constant that is related to the average adsorption energy. The average free energy of adsorption (E) in kJ/mol can be calculated as follows [38]:

$$E = \frac{1}{\sqrt{-2\beta}} \tag{8}$$

2.2. Kinetic studies of adsorption process

The kinetic equations study reaction speed and its effective factors. In this study, pseudo-first-order and Pseudo-second-order kinetic equations were used to analyze data. The linear equations of the kinetics are as in Eqs. (9) and (10):

$$\ln\left(q_e - q_t\right) = \ln\left(q_e - K_1\right) \tag{9}$$

$$\frac{t}{q_t} = \frac{1}{K_2 q_0^2} + \frac{1}{q_0} t \tag{10}$$

where q_e: the concentration of adsorbed fluoride at equilibrium. q_t: the amount of fluoride adsorbed at the adsorbent surface at time t (mg/g), t is the time (min), K_1: constant of pseudo-first-order equation (1/min), and K_2: constant of pseudo-second-order equation (g/mg/min) [39].

2.3. Intraparticle diffusion rate

2.3.1. Thermodynamics of the adsorption process

The following relation was used to study the thermodynamics of the adsorption process (Eq. (11)).

$$\Delta G = -RT\left(\ln K_C\right) \tag{11}$$

where ($\Delta G°$) is the expression of Gibbs free energy (KJ/mol). R is the universal gas constant (8.314 J/mol/K) and T represents absolute temperature (K). The following relationships were used to calculate the standard enthalpy ($\Delta H°$), standard entropy ($\Delta S°$) in the adsorption process (Eqs. (12) and (13)):

$$\ln K_C = \frac{\Delta S°}{R} - \frac{\Delta H°}{RT} \tag{12}$$

$$K_C = \frac{q_e}{C_e} \tag{13}$$

where K_C (L/g): the ratio of the amount of adsorbed substance per adsorbent (mg/g) to the amount of residue in solution (mg/L) [40].

3. Results and discussion

3.1. Characterization of adsorbent

X-ray diffraction (XRD) pattern and scanning electron microscope (SEM) image were used to study the adsorbent properties. In the XRD pattern, XRD was used to determine the crystalline and non-crystalline adsorption phase. The crystalline phase, the nanoparticles SiO_2 glass (amorphous) is that shown in Fig. 1.

The SEM image was also used to obtain information about the particle surface morphology. According to the image, the size of the nanoparticles is between 31 and 48 nm (Fig. 2).

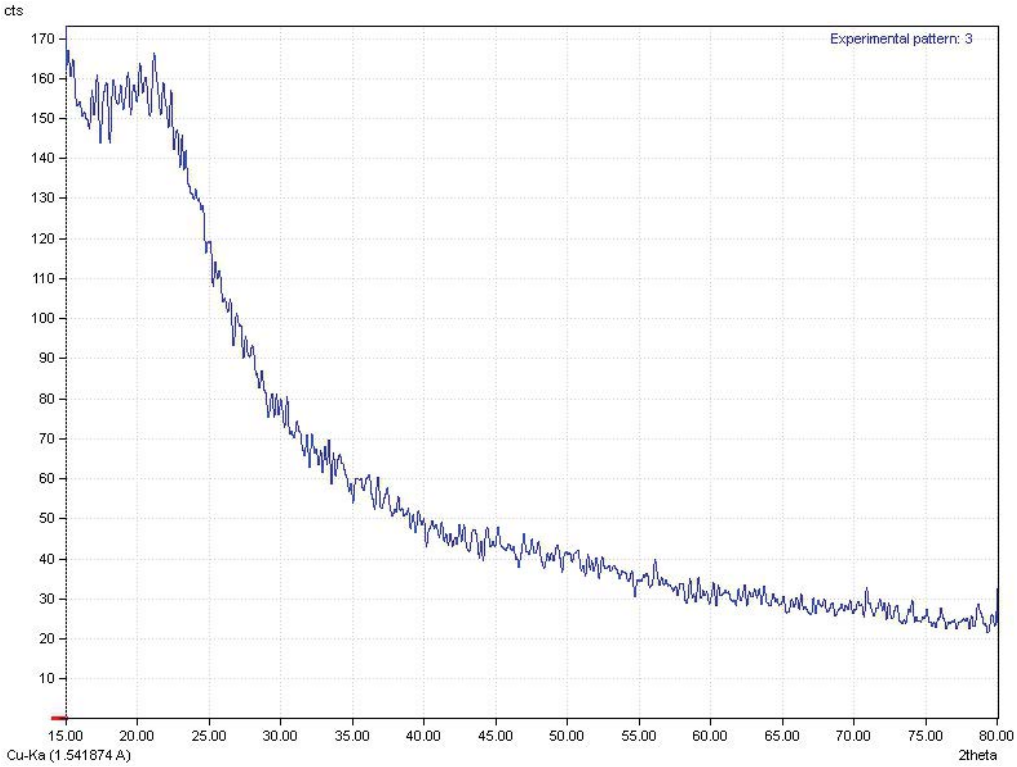

Fig. 1. XRD spectra of silica nanoparticles.

Fig. 2. SEM image of silica nanoparticles.

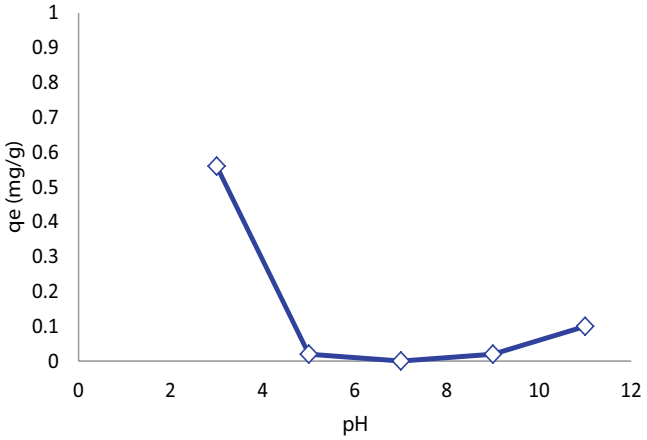

Fig. 3. Effect of pH on removal of fluoride by silica nanoparticles (adsorbent dose = 0.5 g/L, concentration of fluoride = 1 mg/L, and contact time = 60 min).

3.2. The effect of solution pH

In the study, the effect of pH on fluoride removal efficiency was determined by changing the acidity of the environment at pH 3–11, shown in Fig. 3. According to the figure, the highest fluoride removal capacity occurred at the pH = 3 and the adsorbent capacity in these conditions is 0.56 mg/g. And with increasing pH, fluoride adsorption by silica was reduced. Therefore, pH of 3 was chosen as the optimum pH for the next stages.

Observations indicate that the best pH for fluoride removal is pH = 3, since the number of H^+ ions in the acidic medium increases and, by attaching to the adsorbent surface and inducing positive charge, causes more fluoride anions to be adsorbed. Also, at the alkaline pH, OH^- ion, as a competitor causes electrostatic repulsion force between adsorbent and the fluoride anions and the fluoride anions takes place and occupies some adsorbent sites, and as a result, the fluoride adsorption decreases [41,42]. In a study by Jagtap et al. [43] on fluoride removal, adsorption of fluoride by adsorbent in acidic environments was found to be superior to alkaline [43]. In another study by Liang and Luo [44], SiO_2 adsorbent used to remove humic acid, acidic pHs have higher removal efficiency [44].

3.3. Effect of adsorbent dosage

At this stage, the effect of different adsorbent doses (0.2, 0.5, 1, 1.5, and 2 g/L) on the amount of fluoride removal by silica nanoparticles was investigated. Fig. 4 shows the effect of adsorbent doses, it is known that the maximum adsorption capacity of silica is 0.2 g/L and decreases its adsorption capacity by increasing the amount of adsorbent dose. As a result, the optimum dose of adsorbent in this study was 0.2 g/L with an adsorption capacity of 1.10 mg/g.

The results of the effect of the removal of fluoride by various amounts of silica nanoparticles in Fig. 4 show that the highest adsorption capacity of 0.2 g/L is 1.1 mg/g. By increasing the adsorbent dose, the amount of fluoride adsorbed per gram of adsorbing mass decreases due to the lack of saturation of the active sites in the fluoride adsorption. This means that by increasing the adsorbent dose, the total capacity of the active sites on the adsorbent is not used and it reduces the amount of adsorption per gram of adsorbent [45]. The results of this study are in accordance with a study by Naghizadeh et al. [3].

3.4. Effect of contact time and initial concentration of fluoride

The results of the effect of contact time and fluoride concentration on removal of fluoride by silica nanoparticles were investigated, and Fig. 5 shows the results of this stage. For this purpose, various concentrations of fluoride (2, 5, 8, and 10 mg/L) were prepared and experiment at contact times of 2–120 min. As shown in this figure, with increasing fluoride concentration, the adsorption capacity has increased. Also, fluoride was removed rapidly for 10 min, after which the process of change was almost constant. The adsorption capacity at 10 min for concentrations of 2, 5, 8, and 10 mg/L was 1.55, 4.20, 7.7, and 8.05 mg/g, respectively.

Observations show that as the contact time increases by up to 10 min, the adsorption capacity is ascending, and as the contact time increases, the adsorption capacity remains almost constant, which may be due to a decrease in the concentration of soluble fluoride and a decrease in adsorption capacity, because in the initial stages adsorption of more porosity and more porosity is available at the adsorbent surface, resulting in a higher level of adsorbing material, and over time, these spaces are occupied by fluoride molecules.

Also, the results of different concentrations of fluoride show that increasing the fluoride concentration also increases the adsorption capacity. Fig. 5 shows that at 10 min, with increasing fluoride concentration from 2 to 10 mg/L fluoride, the amount of adsorption capacity ranged from 1.55 to 8.05 mg/g. The reason for this is that with increasing fluoride concentration, the fluoride ions around the adsorbent increased and the possibility of collision between the adsorbent and fluoride molecules increased and, as a result, increased adsorption of fluoride by adsorbent [46]. A study conducted by Viswanathan and Meenakshi reported that fluoride removal was rapid in the first 40 min, followed by a constant amount, and also reported an increase in fluoride uptake by increasing fluoride concentration [47].

3.5. Adsorption isotherms

The results of the fluoride adsorption study on silica nanoparticles from various isotherms are reported in Table 1. As shown in this table, the process of removal fluoride by silica nanoparticles more than Dubinin–Radushkevich, Temkin, Langmuir, and Freundlich isotherms.

According to the results of Table 1, it is shown that according to the low regression coefficient (R^2 = 0.9), fluoride adsorption by silica nanoparticles is less than Langmuir isotherm. Also in the Langmuir model, the maximum fluoride adsorption capacity (q_{max}) on silica nanoparticles 16 mg/g is obtained, which differs greatly from the equilibrium capacity obtained in the experiments. The amount of K_L to adsorb fluoride on silica nanoparticles is 0.05. K_L is a constant value that its size is directly related to the size of the adsorbent molecules [34].

Also, fluoride adsorption behavior on silica nanoparticles was investigated using a parameter (R_L) derived from the Langmuir model. If this parameter is equal to zero, adsorption is irreversible and when the value of this parameter is located between zero and one, adsorption is desirable, and if R_L is equal to 1, adsorption is linear, and if the R_L is greater than 1, adsorption is undesirable. According to the results of the Langmuir isotherm for fluoride intake R_L on the adsorbent is located between 0 and 1 is therefore desirable adsorption of fluoride on silica nanoparticles

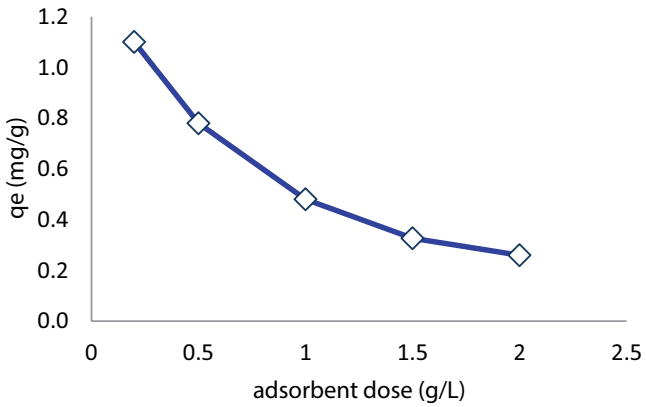

Fig. 4. Effect of adsorbent dosage on removal of fluoride by silica nanoparticles (pH = 3, concentration of fluoride = 1 mg/L, and contact time = 60 min).

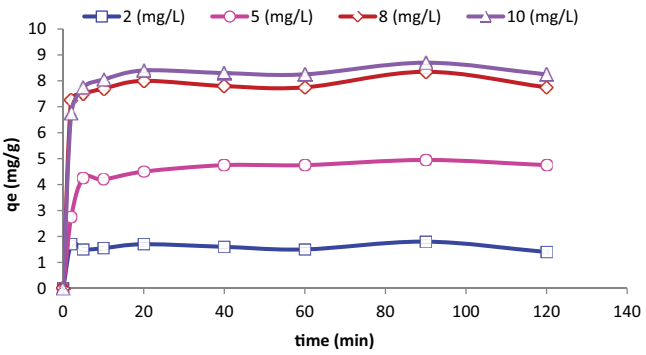

Fig. 5. Effect of fluoride initial concentrations and different contact times on silica nanoparticles adsorption capacities (pH = 3 and adsorbent dose = 0.5 g/L).

Table 1
Regression constants and coefficients of fluoride adsorption isotherms by silica nanoparticles

Isotherms	Constants	Values
Langmuir	q_{max} (mg/g)	16.00
	K_L (L/mg)	0.05
	R_L	0.50
	R^2	0.90
Freundlich	k_F (mg/g)	1.06
	$1/n$	1.01
	n	0.99
	R^2	0.89
BET	$1/A.Xm$	19.26
	$(A^{-1})/(A.Xm)$	25.29
	A	488.20
	Xm	19.30
	R^2	0.38
Temkin	A_T (L/mg)	0.86
	b_T	583.44
	B	4.25
	R^2	0.96
Dubinin–Radushkevich	β (mol²/kJ²)	0.00
	E (kJ/mol)	0.57
	q_m (mg/g)	9.32
	R^2	1.00

[48,49]. Regarding the results obtained from the Freundlich isotherm, the regression coefficient (R^2) is 0.89, which is less than R^2 in the Langmuir isotherm. The amount of K_F in silica nanoparticles is equal to 1.06 (mg/g) (mg/L)^n. The $1/n$ parameter decreases by increasing the adsorption capacity of the adsorbent. The amount of $1/n$ in silica nanoparticles is 1.01.

The results from Table 1 show that the BET isotherm regression coefficient is less than and equal to 0.38 for Langmuir and Freundlich isotherms. As a result, the adsorption of fluoride by adsorbent does not obey this isotherm.

According to Table 1, the regression coefficient for isothermic admixture in fluoride adsorption by the silica nanoparticles is equal to 0.96, which is greater than the regression coefficients of Langmuir, Freundlich, and BET isotherms. As a result, this isotherm has a better description of adsorbing fluoride by the desired adsorbent.

The results of Table 1 show that the adsorption process is based on the regression coefficient in the Dubinin–Radushkevich isotherm equal to 1, which is higher than other isotherms. Therefore, with regard to the correlation coefficients, it can be concluded that the process of fluoride adsorption by silica nanoparticles is entirely consistent with the Dubinin–Radushkevich isotherm. In a study by Kır et al. [50], fluoride removal reported that adsorption behavior was consistent with Dubinin–Radushkevich and Freundlich isotherms [50].

3.6. The kinetics of the adsorption process

Also, in the study, pseudo-first and pseudo-second-order kinetics were investigated and the adsorption process for this adsorbent is more correlated with quadratic kinetics, the results of which are shown in Table 2 and Figs. 6 and 7.

Kinetic studies in all adsorption processes are an important parameter in the design of experiments. Table 2 shows the results of the study of the kinetic parameters of the study. As shown in the table, the values of the regression coefficient for fluoride in relation to the pseudo-second-order model show that the adsorption of fluoride by silica nanoparticles follows this model. As can be seen in the table, the experimental adsorption capacity values (q_e, cal) calculated in the pseudo-second-order model is closer to the test adsorption capacity values (q_e,exp) than the pseudo-first-degree model. In a study by Ma et al., it was reported that fluoride removal on magnetic chitosan follows pseudo-second-degree kinetics [51].

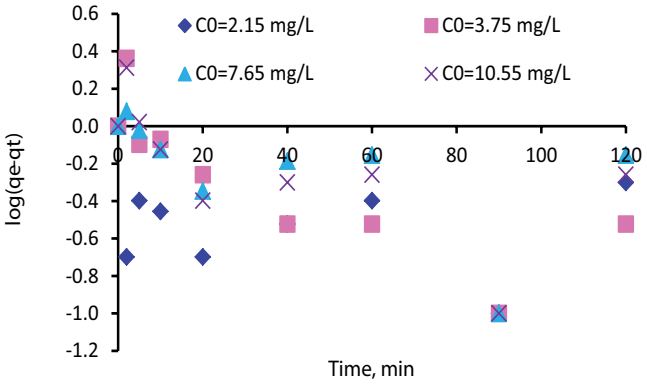

Fig. 6. Pseudo-first-order kinetic for the fluoride adsorption onto silica nanoparticles.

Table 2
Results of kinetic calculations for fluoride removal by silica nanoparticles

C_0 (mg/L)	Pseudo-first-order			Pseudo-second-order			$q_e$exp (mg/g)
	K_1 (min^{-1})	$q_e$cal (mg/g)	R^2	K_2 (g/mg min)	$q_e$cal (mg/g)	R^2	
2.15	0.00	0.36	0.04	0.52	1.50	0.98	1.90
3.75	0.02	0.98	0.64	0.22	4.85	1.00	5.05
7.65	0.01	0.88	0.29	1.35	7.93	1.00	8.45
10.55	0.01	0.96	0.41	0.52	8.40	1.00	8.80

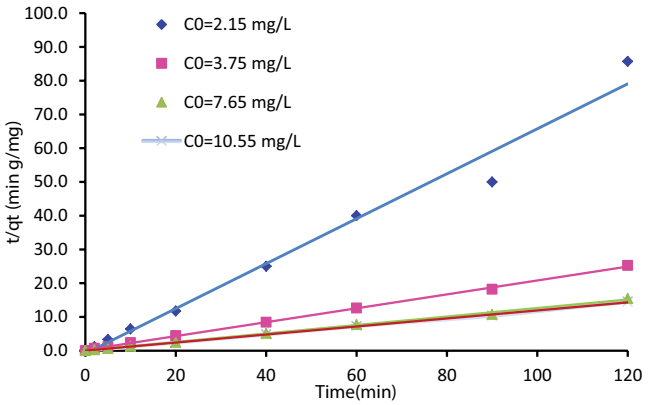

Fig. 7. Pseudo-second-order kinetic for the fluoride adsorption onto silica nanoparticles.

3.7. Intraparticle diffusion rate

The values of "*a*" and K_{id} illustrate the adsorption mechanism and the adsorption factor, respectively [52]. Table 3 shows the values of intraparticle diffusion.

By increasing the initial concentration of fluoride, the amount of *c* increases which indicates an increase in the adsorption rate. Also, the value of "*a*" indicates the process is better [53].

3.8. Effect of temperature process on removal of fluoride and determination of thermodynamics parameters

The effect of the solution temperature on different temperatures (283K, 293K, 303K, and 313K) on the efficiency of fluoride removal by silica nanoparticles was investigated by fixing other parameters. The results are shown in Fig. 8.

Table 4 shows the values obtained from the thermodynamic studies of this study. According to the table, the values of standard enthalpy $\Delta H°$ and standard entropy $\Delta S°$ are positive and respectively, 38.41 (kJ/mol) and 130.3 (J/mol K). The positive values of these two parameters indicate that the fluoride adsorption process was heated by silica nanoparticles and that the reaction temperature increased with increasing adsorption capacity. Also, the negative trend of Gibbs free energy ($\Delta G°$) in this study shows that the fluoride adsorption process is spontaneous by silica nanoparticles. In a study by Jactab et al. was conducted on a modified chitosan, enthalpy and entropy values were standard and positive and the amount of free energy was negative, which indicates spontaneous endothermic process to remove fluoride[46].

Table 3
Intraparticle diffusion rate constants at different initial concentrations

C_0 (mg/L)	K_{id} (mg/g min$^{0.5}$)	*a*
2.15	0.12	0.05
3.75	0.28	0.24
7.65	0.49	0.26
10.55	0.48	0.27

Table 4
Calculations of thermodynamics parameters for the fluoride adsorption onto silica nanoparticles

T (K)	q_e (mg/g)	Thermodynamics parameters		
		ΔG (kJ/mol)	ΔH (kJ/mol)	ΔS (J/mol K)
283	4.5	1.72	38.41	130.30
293	9	–0.15		
303	11.25	–0.86		
313	12.75	–1.31		

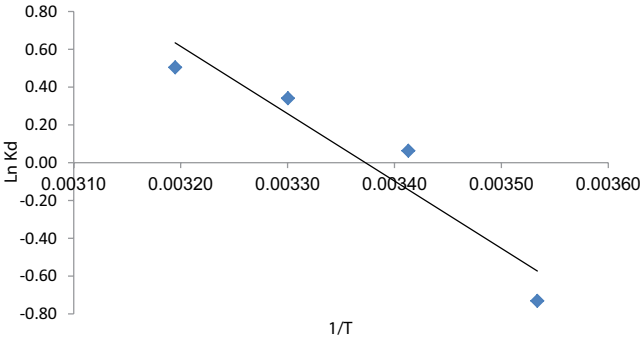

Fig. 8. Effect of temperature and thermodynamics survey on removal of fluoride by silica nanoparticles.

Table 5
Adsorption capacities of the studied adsorbents

Adsorbent	Maximum adsorption capacity (mg/g)	References
Silica nanoparticle	8.05	This study
Bentonite	5.5	[3]
Montmorillonite	4.5	[3]
Activated carbon (Morringa Indica)	0.23	[54]
Nanochitosan	9.4	[4]
Biomass	39.9	[55]
Graphene	17.65	[56]
Hydrous bismuth oxides	1.93	[57]

3.9. Comparison between silica nanoparticles used in the present study with other adsorbents

The comparison of adsorption capacity of silica nanoparticle with other adsorbent was shown in Table 5. Regarding to this table, the adsorption capacity of biomass, graphene, and nanochitosan was higher than the studied adsorbent and the other adsorbents have the lower adsorption capacities.

4. Conclusion

This study showed that silica nanoparticles in optimum conditions can be used as an effective, usable, and inexpensive adsorbent for removal of fluoride ions from fluoride-containing solutions, which have higher concentration than

the standard values. In optimum conditions (pH = 3, the adsorbent dose of 0.2 g/L, the contact time of 10 min, and the initial fluoride concentration of 10 mg/L) the maximum adsorption capacity (q_{max}) were found to be 8.40 mg/g. Also, adsorption process follows the Dubinin–Radushkevich isotherm and pseudo-second-order kinetics, and the reaction was spontaneous endothermic.

Acknowledgment

This study has resulted from the research project funded by Birjand University of Medical Sciences (BUMS). The authors are grateful for the financial support provided by research deputy of BUMS.

References

[1] W.H. Organization, Guidelines for Drinking-Water Quality: Recommendations, 1(2004) 375.
[2] R. Maheshwari, Fluoride in drinking water and its removal, J. Hazard. Mater., 137 (2006) 456–463.
[3] A. Naghizadeh, K. Gholami, Bentonite and montmorillonite nanoparticles effectiveness in removal of fluoride from water solutions, J. Water Health., 15 (2017) 555–565.
[4] A. Naghizadeh, H. Shahabi, E. Derakhshani, F. Ghasemi, A.H. Mahvi, Synthesis of nanochitosan for the removal fluoride from aqueous solutions: a study of isotherms, kinetics, and thermodynamics, Fluoride, 50 (2017) 256–268.
[5] W.H. Organization, Guidelines for Drinking-Water Quality [Electronic Resource]: Incorporating 1st and 2nd Addenda, Recommendations, 1 (2008) 375.
[6] S.M. Prabhu, S. Meenakshi, Synthesis of metal ion loaded silica gel/chitosan biocomposite and its fluoride uptake studies from water, J. Water Process Eng., 3 (2014) 144–150.
[7] N. Chinoy, Effects of fluoride on physiology of animals and human beings, Indian J Environ Toxicol., 1 (1991) 17–32.
[8] A. Wang, T. Xia, Q. Chu, M. Zhang, F. Liu, X. Chen, K. Yang, Effects of fluoride on lipid peroxidation, DNA damige and apoptosis in human embryo hepatocytes, BES, 17 (2004) 217–222.
[9] P. Miretzky, A.F. Cirelli, Fluoride removal from water by chitosan derivatives and composites: a review, J. Fluor Chem., 132 (2011) 231–240.
[10] S.S. Tripathy, J.L. Bersillon, K. Gopal, Removal of fluoride from drinking water by adsorption onto alum-impregnated activated alumina, Sep. Purif. Technol., 50 (2006) 310–317.
[11] N. Viswanathan, S. Meenakshi, Enriched fluoride sorption using alumina/chitosan composite, J. Hazard. Mater., 178 (2010) 226–232.
[12] N. Chen, Z. Zhang, C. Feng, N. Sugiura, M. Li, R. Chen, Fluoride removal from water by granular ceramic adsorption, J. Colloid Interface Sci., 348 (2010) 579–584.
[13] G. Asgari, B. Roshani, G. Ghanizadeh, The investigation of kinetic and isotherm of fluoride adsorption onto functionalize pumice stone, J. Hazard. Mater., 217 (2012) 123–132.
[14] B. Kemer, D. Ozdes, A. Gundogdu, V.N. Bulut, C. Duran, M. Soylak, Removal of fluoride ions from aqueous solution by waste mud, J. Hazard. Mater., 168 (2009) 888–894.
[15] M. Sujana, R. Thakur, S. Rao, Removal of fluoride from aqueous solution by using alum sludge, J. Colloid Interface Sci., 206 (1998) 94–101.
[16] M. Tahaikt, I. Achary, M. Sahli, Z. Amor, M. Taky, A. Alami, A. Boughriba, M. Hafsi, A. Elmidaoui, Defluoridation of Moroccan groundwater by electrodialysis: continuous operation, Desalination, 189 (2006) 215–220.
[17] M. Arora, R.C. Maheshwari, S.K. Jain, A. Gupta, Use of membrane technology for potable water production, Desalination, 170 (2004) 105–112.
[18] K. Hu, J.M. Dickson, Nanofiltration membrane performance on fluoride removal from water, J. Membr. Sci., 279 (2006) 529–538.
[19] M.H. Omidi, F.N. Azad, M. Ghaedi, A. Asfaram, M.H.A. Azqhandi, L. Tayebi, Synthesis and characterization of Au-NPs supported on carbon nanotubes: application for the ultrasound-assisted removal of radioactive UO_2^{2+} ions following complexation with Arsenazo III: spectrophotometric detection, optimization, isotherm and kinetic study, J. Colloid Interface Sci., 504 (2017) 68–77.
[20] A. Asfaram, M. Ghaedi, H. Abidi, H. Javadian, M. Zoladl, F. Sadeghfar, Synthesis of Fe_3O_4@ CuS@ Ni_2P-CNTs magnetic nanocomposite for sonochemical-assisted sorption and preconcentration of trace Allura Red from aqueous samples prior to HPLC-UV detection: CCD-RSM design, Ultrason. Sonochem., 44 (2018) 240–250.
[21] F.L. Mi, S.J. Wu, F.M. Lin, Adsorption of copper (II) ions by a chitosan–oxalate complex biosorbent, Int. J. Biol. Macromol., 73 (2015) 136–144.
[22] E. Sharifpour, H.Z. Khafri, M. Ghaedi, A. Asfaram, R. Jannesar, Isotherms and kinetic study of ultrasound-assisted adsorption of malachite green and Pb^{2+} ions from aqueous samples by copper sulfide nanorods loaded on activated carbon: experimental design optimization, Ultrason. Sonochem., 40 (2018) 373–382.
[23] Xu, X., X. Xu, Q. Li, H. Cui, J. Pang, L. Sun, H. An, J. Zhai, Adsorption of fluoride from aqueous solution on magnesia-loaded fly ash cenospheres, Desalination, 272 (2011) 233–239.
[24] S. Vinitnantharat, S. Kositchaiyong, S. Chiarakorn, Removal of fluoride in aqueous solution by adsorption on acid activated water treatment sludge, Appl. Surface Sci., 256 (2010) 5458–5462.
[25] G. Asgari, A.R. Rahmani, J. Faradmal, A.M. Seid Mohammadi, Kinetic and isotherm of hexavalent chromium adsorption onto nano hydroxyapatite, JRHS, 12 (2012) 45–53.
[26] A. Asfaram, M. Ghaedi, K. Dashtian, G.R. Ghezelbash, Preparation and characterization of Mn0. 4Zn0. $6Fe_2O_4$ nanoparticles supported on dead cells of Yarrowia lipolytica as a novel and efficient adsorbent/biosorbent composite for the removal of azo food dyes: central composite design optimization study, ACS Sustain, Chem. Eng., 6 (2018) 4549–4563.
[27] J. Lu, Y. Li, X. Yan, B. Shi, D. Wang, H. Tang, Sorption of atrazine onto humic acids (HAs) coated nanoparticles, Colloids Surface Physicochem. Eng. Aspects, 347 (2009) 90–96.
[28] J. Zhai, X. Tao, Y. Pu, X.F. Zeng, J.F. Chen, Core/shell structured ZnO/SiO_2 nanoparticles: preparation, characterization and photocatalytic property, Appl. Surface Sci., 257 (2010) 393–397.
[29] T. Moriguchi, K. Yano, M. Tahara, K. Yaguchi, Metal-modified silica adsorbents for removal of humic substances in water, J. Colloid Interface Sci., 283 (2005) 300–310.
[30] S. Syed, M. Alhazzaa, M. Asif, Treatment of oily water using hydrophobic nano-silica, Chem. Eng. J., 167 (2011) 99–103.
[31] S. Banerjee, J. Das, R.P. Alvarez, S. Santra, Silica nanoparticles as a reusable catalyst: a straightforward route for the synthesis of thioethers, thioesters, vinyl thioethers and thio-Michael adducts under neutral reaction conditions, NJC, 34 (2010) 302–306.
[32] E. Derakhshani, A. Naghizadeh, Ultrasound regeneration of multi wall carbon nanotubes saturated by humic acid, Desal. Wat. Treat., 52 (2014) 7468–7472.
[33] A. Naghizadeha, F. Momenia, E. Derakhshania, Efficiency of ultrasonic process in regeneration of graphene nanoparticles saturated with humic acid, Desal. Wat. Treat., 70 (2017) 290–293.
[34] A. Naghizadeh, Comparison between activated carbon and multiwall carbon nanotubes in the removal of cadmium (II) and chromium (VI) from water solutions, J. Water Supply Res. T., 64 (2015) 64–73.
[35] A. Asfaram, M. Ghaedi, A. Goudarzi, M. Rajabi, Response surface methodology approach for optimization of simultaneous dye and metal ion ultrasound-assisted adsorption onto Mn doped Fe_3O_4-NPs loaded on AC: kinetic and isothermal studies, Dalton Trans., 44 (2015) 14707–14723.
[36] A. Naghizadeh, R. Nabizadeh, Removal of reactive blue 29 dye by adsorption on modified chitosan in the presence of hydrogen peroxide, Environ. Prot. Eng., 42(2016) 149–168.
[37] M. Özacar, İ.A. Şengil, Adsorption of metal complex dyes from aqueous solutions by pine sawdust, Bioresour. Technol., 96 (2005) 791–795.

[38] A. Şeker, T. Shahwan, A.E. Eroğlu, S. Yılmaz, Z. Demirel, M.C. Dalay, Equilibrium, thermodynamic and kinetic studies for the biosorption of aqueous lead (II), cadmium (II) and nickel (II) ions on Spirulina platensis, J Hazard Mater., 154 (2008) 973–980.
[39] A. Naghizadeh, M. Ghafouri, A. Jafari, Investigation of equilibrium, kinetics and thermodynamics of extracted chitin from shrimp shell in reactive blue 29 (RB-29) removal from aqueous solutions, Desal. Wat. Treat., 70 (2017) 355–363.
[40] A. Naghizadeh, H. Shahabi, F. Ghasemi, A. Zarei, Synthesis of walnut shell modified with titanium dioxide and zinc oxide nanoparticles for efficient removal of humic acid from aqueous solutions, J. Water Health., 14 (2016) 989–997.
[41] N.N. Nassar, Rapid removal and recovery of Pb (II) from wastewater by magnetic nanoadsorbents, J. Hazard. Mater., 184 (2010) 538–546.
[42] O. Gutierrez-Muñiz, G. García-Rosales, E. Ordoñez-Regil, M.T. Olguin, A. Cabral-Prieto, Synthesis, characterization and adsorptive properties of carbon with iron nanoparticles and iron carbide for the removal of As (V) from water, J. Environ. Manage., 114 (2013) 1–7.
[43] S. Jagtap, D. Thakre, S. Wanjari, S. Kamble, N. Labhsetwar, S. Rayalu, Synthesis and characterization of lanthanum impregnated chitosan flakes for fluoride removal in water, Desalination, 273 (2011) 267–275.
[44] L. Liang, L. Luo, S. Zhang, Adsorption and desorption of humic and fulvic acids on SiO_2 particles at nano-and micro-scales, Colloids Surface Physicochem. Eng. Aspects, 384 (2011) 126–130.
[45] K.V. Kumar, K. Porkodi, Mass transfer, kinetics and equilibrium studies for the biosorption of methylene blue using Paspalum notatum, J. Hazard. Mater., 146 (2007) 214–226.
[46] S. Jagtap, M.K. Yenkie, S. Das, S. Rayalu, New modified chitosan-based adsorbent for defluoridation of water, J. Colloid Interface Sci., 332 (2009) 280–290.
[47] N. Viswanathan, S. Meenakshi, Enhanced fluoride sorption using La (III) incorporated carboxylated chitosan beads, J. Colloid Interface Sci., 322 (2008) 375–383.
[48] J. Su, H.F. Lin, Q.P. Wang, Z.M. Xie, Z.L. Chen, Adsorption of phenol from aqueous solutions by organomontmorillonite, Desalination, 269 (2011) 163–169.
[49] Y. Ho, J. Porter, G. McKay, Equilibrium isotherm studies for the sorption of divalent metal ions onto peat: copper, nickel and lead single component systems, Water Air Soil Pollut., 141 (2002) 1–33.
[50] E. Kır, H. Oruc, I. Kır, T. Sardohan-Koseoglu, Removal of fluoride from aqueous solution by natural and acid-activated diatomite and ignimbrite materials, Desal. Wat. Treat., 57 (2016) 21944–21956.
[51] W. Ma, F.Q. Ya, M. Han, R. Wang, Characteristics of equilibrium, kinetics studies for adsorption of fluoride on magnetic-chitosan particle, J. Hazard. Mater., 143 (2007) 296–302.
[52] E. Demirbas, M. Kobya, E. Senturk, T. Ozkan, Adsorption kinetics for the removal of chromium (VI) from aqueous solutions on the activated carbons prepared from agricultural wastes, Water SA, 30 (2004) 533–539.
[53] A. Naghizadeh, S. Nasseri, A.M. Rashidi, R.R. Kalantary, R. Nabizadeh, A.H. Mahvi, Adsorption kinetics and thermodynamics of hydrophobic natural organic matter (NOM) removal from aqueous solution by multi-wall carbon nanotubes, Water Sci. Technol. Water Supp., 13 (2013) 273–285
[54] J. Karthikeyan, I.S. Siva, Flouride sorption using morringa indica-based activated carbon, Iranian J. Environ. Health Sci. Eng., 4 (2007) 21–28.
[55] P.K. Pandey, M. Pandey, R. Sharma, Defluoridation of water by a biomass: *Tinospora cordifolia*, JEP, 3 (2012) 610.
[56] Y. Li, P. Zhang, Q. Du, X. Peng, T. Liu, Z. Wang, Y. Xia, W. Zhang, K. Wang, H. Zhu, Adsorption of fluoride from aqueous solution by graphene, J. Colloid Interface Sci., 363 (2011) 348–354.
[57] T. Ishihara, Y. Shuto, S. Ueshima, H.L. Ngee, H. Nishiguchi, Y. Takita, Titanium hydroxide as a new inorganic fluoride ion exchanger, J. Ceram Soc. Jpn., 110 (2002) 801–803.